In Vivo Oxygen Transport in the Normal Rabbit Femoral Arterial Wall

DONALD W. CRAWFORD, LLOYD H. BACK, and MARK A. COLE, with the technical assistance of CYRIL FELDSTEIN and WENDELIN J. PAULE, *Department of Medicine, Cardiology Division, University of Southern California School of Medicine, Los Angeles, California 90033; and Jet Propulsion Laboratory, Pasadena, California 91103*

ABSTRACT In vivo measurements of tissue oxygen tension were made at 10-μm intervals through functioning *in situ* rabbit femoral arterial walls, using inhalation anesthesia and recessed microcathodes with ~4-μm external diameters. External environment was controlled with a superfusion well at 30 torr P_{O_2}, 35 torr P_{CO_2}. Blood pressure, gas tension levels, and blood pH were held within the normal range. Radial P_{O_2} measurements closely fit a mathematical model for unidimensional diffusion into a thick-walled artery with uniform oxygen consumption, and the distances traversed fit measured dimensions of quick-frozen in vivo sections. Using standard values for diffusion and solubility coefficients, mean calculated medial oxygen consumption was 99 nl_0/ml-s. Mural oxygen consumption appeared to be related linearly to mean tangential wall stress. Differences in experimental design and technique were compared with previous in vivo and in vitro measurements of wall oxygenation, and largely account for the varying results obtained. Control of environment external to the artery, and maintenance of normally flowing blood in the lumen in vivo appeared critical to an understanding of mural oxygenation in life. If the conditions of this experiment prevailed in arteries with thicker avascular layers, P_{O_2} could have been 20 torr at ~156 μm and 10 torr at 168 μm from blood (average values).

INTRODUCTION

Evidence has accumulated that portions of the walls of some arteries have limited oxygen availability. Adams and Bayliss noted that intimal thickening with advancing age was associated with enzyme loss in the middle regions of the tunica media, presumably caused by relatively small increases in distance for diffusion (1). Lehninger also suggested that the relatively thick media interposed an extended path for diffusion of oxygen to the cells (2). From the results of a series of studies with arterial wall enzymes and isoenzymes, Zemplenyi (3) has suggested a mid-zone adaptation to hypoxia.

In view of past evidence that a considerable amount of the energy required by the arterial wall could be derived from glycolysis (2, 4), the level of oxygenation necessary to maintain cellular processes adequately has been unclear. Recent evidence suggests that aerobic metabolism meets a larger percentage of the energy requirement of the wall than earlier references indicated (5). Hypoxia produces arterial injury and accelerates atherosclerosis in rabbits. The effect of carbon monoxide is less clear (6, 7). Direct measurements of arterial wall oxygenation seem indicated, and a few have been undertaken.

In 1968, Moss et al. (8) used a sharply cut, bare platinum wire cathode (125 μm diameter) for measurement of oxygen current in vivo in exposed dog femoral arteries. There was a progressive fall in current from adventitia toward intima, but an abrupt, essentially discontinuous, rise on entering the blood stream. When the vessel was excised and autografted, current rose progressively from adventitia to blood stream. In 1973, Niinikoski et al. (9) used a sharply tapered platinum microcathode. The tip was covered with a membrane so that P_{O_2} could be approximated from oxygen current. In vivo punctures were made into rabbit abdominal aorta through a drop of mineral oil. Again there was a biphasic response with a mid-medial minimum in P_{O_2} and an abrupt rise on entering the blood stream.

A large oxygen gradient, apparently distributed over a few microns in the region of the intima was found under normal conditions by these investigators. It

This work was presented in part at the 51st Scientific Sessions of the American Heart Association, 13–16 November 1978.

Received for publication 27 April 1979 and in revised form 14 January 1980.

clearly suggests a transport barrier for oxygen in this region in relation to the level of medial oxygen consumption. Subsequent in vitro measurements of wall oxygenation have not confirmed the presence of such a barrier (10, 11). No transport theory modeling was used in the in vivo studies of Moss et al. (8) or Niinikoski et al. (9) and in vivo oxygen consumptions were not calculated.

In the interval, an improved microcathode design for in vivo tissue studies has appeared (12, 13). We report here a reexamination of the oxygenation of an in vivo artery, the rabbit femoral, using this microcathode system, with further precautions to control the periarterial P_{O_2} environment and to prevent tissue compression. Diffusional theory has been applied, and in vivo medial oxygen consumptions have been determined in each case on this basis. A previous report from this laboratory on prior experiments has discussed earlier technique, mural oxygen tension levels, and application of the thin wall diffusional model (14).

METHODS

Electrode fabrication and calibration. The electrodes were fabricated according to the method described by Whalen (12), with slight modifications. Glass capillaries were filled with Wood's alloy and pulled to form a metal-filled tip of ~0.5 μm in diameter. The tips were beveled to a 30°–40° angle on a rotating drum covered with diamond dust, yielding points expanding to 2–4 μm at the bases of the bevels. The electrodes were then siliconized and dried. The Wood's alloy was electrically etched to form a tip recess, and gold was plated onto the end of the Wood's alloy column. The remaining recess, 5–20 μm, was filled with hydroxymethacrylate hydrogel (Spectra Research Labs, Arcadia, Calif.) and hydrated. This hydrogel produced more stable performance and less "poisoning" than previous fillers. The performance of electrodes of this configuration, as well as other types, has been analyzed by Schneiderman and Goldstick (15). The recess dimensions we chose were such that there should be a negligible diffusion field caused by the electrode outside the recess. In practice, our electrodes were very stable, demonstrated no stirring artefact, and were relatively insensitive to changes in temperature. When the same gas mixture was equilibrated with buffer at various temperatures, changes in oxygen current were seen equivalent to 0–2 torr/°C.

Each electrode was checked for a plateau of stable current in its polarographic curve and initial calibration was performed at the plateau polarizing voltage so determined, usually 0.7–0.8 V negative with respect to a chloridized silver wire anode. Solutions of bicarbonate-buffered balanced electrolyte solution (BBS[1] [16]) were equilibrated at ~40°C with oxygen at 30, 90, and 140 torr in nitrogen and ~5% carbon dioxide, and allowed to flow through a well into which the electrodes were introduced for calibration; pH measured 7.32–7.40. The calibration temperature was chosen arbitrarily as that of the average animal rectal temperature during the experiments. The current vs. P_{O_2} response was linear between 0 and 150 torr, and standard deviation from the regression varied from 0 to 4 torr. Average signal amplitude was 0.36 pA/torr, as measured with a Keithley 417 picoammeter (Keithley Instruments, Inc., Cleveland, Ohio) and recorded on a strip chart.

Experimental procedure. Light anesthesia was induced and maintained in New Zealand white rabbits, weighing 3–5 kg, using an oxygen-nitrous oxide 0.1–0.3% methoxyflurane mixture. Electrode response is not affected by this anesthesia (17). Inspired oxygen was regulated between 20 and 25% to maintain relatively normal Pa_{O_2}. An elastic abdominal binder and a support above the inguinal ligament were used to prevent transmission of respiratory motion from the abdomen to the femoral artery. The femoral artery was exposed surgically, because of its position somewhat posterior (dorsal) to the femoral vein in the rabbit, but we attempted to leave the adventitial surface uninjured. A well was formed over the artery by lifting the skin of the incision edges around a soft plastic cuff. An arterial cannula was introduced into the opposite femoral artery, and this incision was used to introduce a large silver-silver chloride anode. The cannula was used with a small displacement strain gauge to continually record arterial blood pressure, and as a source for arterial blood for repeated measurement of blood gas tensions throughout the procedure. Rectal and well temperatures were monitored using thermistor thermometers. BBS (16) with oxygen tensions of 30, 90, and 140 torr at body temperature were continually available to fill the well through a system of pumps and water-jacketed tubing from a large temperature-controlled water bath containing the equilibration flasks. Arterial blood and calibration solution pH and partial pressures were measured initially and between each electrode traverse using a Radiometer PSM-71 (Radiometer Co., Copenhagen, Denmark), with water jackets held at ~40°C. This proved to be a close but not always an exact match of rabbit rectal temperature under our experimental conditions. However, with close matching between the Radiometer water-jacket temperature, calibration solution temperature and rabbit rectal temperature, no correction was necessary for calibration solution gas pressures. Blood partial pressures were corrected to rabbit temperature when necessary using the method of Severinghaus (18).

Considerable evidence exists that electrodes with a relatively long, filled-tip recess show little difference in response when in saline or albumin solutions, and that properly functioning electrodes respond accurately to P_{O_2} in tissue (12, 13). In our experience, the use of hydroxymethacrylate hydrogel as a tip filler considerably improves the fabrication yield of good electrodes. Calibration just before a puncture is usually the same as that just after, and independently measured blood P_{O_2} is accurately predicted. No runs were used when prior and following calibrations did not match.

The experiments were done inside a large Faraday cage from which all alternating current wiring had been excluded. A pneumatically mounted working table was used to exclude vibratory noise, and the animal was fixed on a modified Kopf stereotatic base (David Kopf Instruments, Tujunga, Calif.) that supported a mechanical micromanipulator. A Kopf stepping hydraulic microdrive was used for electrode advances at the micron level after initial positioning of the electrode over the artery with the micromanipulator.

It is difficult to puncture the rabbit femoral artery wall in vivo without indentation of the wall or electrode fracture, as seen under the dissecting microscope. Deformation is not acceptable, particularly because spatial discrimination is necessary for mathematical analysis of the data, and the accompanying tissue compression produces spuriously low P_{O_2} readings. Deformation can usually be avoided by small longi-

[1] *Abbreviations used in this paper*: BBS, bicarbonate-buffered balanced electrolyte solution; j, oxygen flux; w, oxygen consumption.

tudinal vibration of the electrode. Therefore, a miniature loudspeaker was mounted on the microdrive with a machined Lucite rod fixed to the center of the cone, and the electrode mounted on the end of the rod. The loudspeaker was driven at 200–400 Hz during wall punctures, at an amplifier gain sufficient to produce longitudinal electrode motion of ~10 μm in air, considerably less in tissue (19). Tissue compression was avoided in this way and pulsation artefacts were not seen, probably because the electrode surface tethered the arterial wall locally and wall motion was very small at the high heart rates present (~300/min). The essentials of the experimental arrangement are shown schematically in Fig. 1.

After positioning the animal, the well was filled in turn with the three BBS calibration solutions of known P_{O_2} and a calibration was again recorded. Solution was aspirated from the well leaving the exposed arterial surface uncovered, and the electrode was advanced by micron steps during observation with the dissecting microscope, until surface contact was confirmed by appearance of an oxygen current. Before puncture of the wall, the well was again filled with a constantly flowing BBS. Because the contour of the oxygen tension profiles in the rabbit arterial wall is greatly affected by surrounding P_{O_2} (14), all recorded experiments were done with a continuous temperature-equilibrated superfusion of BBS P_{O_2} ~30 torr. This value was selected on the basis of the average P_{O_2} found by electrode advances adjacent to the course of arteries after incision of skin and subcutaneous fat, but without further dissection. Electrode wall traverses were done in 10-μm increments and advancement continued until we obtained a steady value of oxygen current equivalent to previously measured blood P_{O_2} at which time a sample was obtained for blood gas and pH measurement. The electrode was withdrawn in increments into the superfusion solution and recalibrated. For each run, arterial blood pressure was recorded continuously.

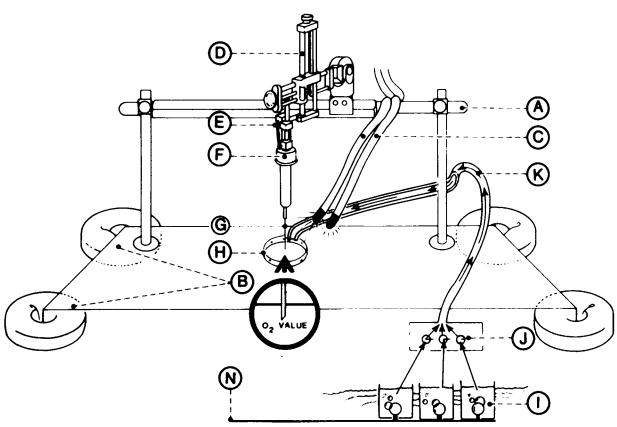

FIGURE 1 Schematic of the experimental facility. The oxygen microcathode (G) is mounted on the cone of a small loudspeaker acting as a vibrator (F). This is fixed to an hydraulic stepping microdrive (E) mounted on a micromanipulator (D). The complete apparatus is supported by a modified stereotactic frame (A) on a heavy base, dampened by pneumatic mounts (B). Superfusion fluids with known P_{O_2} levels (I) equilibrated with animal rectal temperature by heated water bath (N) delivers calibration and environmental stabilizing BBS to a plastic well sutured over the artery (H) through water-jacketed conduits (K). Light is brought into the Faraday cage by fiberoptic bundles (C). The axis of the electrode is perpendicular to the surface of the artery under the well.

Before the termination of most of the experiments, the surface of the artery was cleared of solution by aspiration and this and the surrounding tissues were quick-frozen *in situ* with Freon 22 (Phillips Manufacturing Co., Chicago, Ill.) at −160°C followed by liquid nitrogen. On first exposure to Freon, arterial blood pressure remained at the level present during experimentation. The animal was sacrificed and the tissue block was removed. The tissue was fixed and embedded by a freeze-exchange method (20), sectioned transverse to the arterial axis, and stained with hematoxylin and eosin, or with Verhoeff's or periodic acid-Schiff to facilitate observation of vasa vasorum.

Oxygen transport theory and data analysis. Oxygen current values from the strip chart recordings were converted to oxygen tension values and plotted against depth of puncture. These values were correlated with measurements of adventitial and medial dimensions and vessel radius obtained from examination of the freeze-exchanged sections.

If arterial blood and periarterial P_{O_2} levels, wall dimensions, mural oxygen consumption, and diffusion coefficients are constant over the time interval and area measured, and diffusion is unidimensional, then the appropriate diffusion equation can be solved, and the measured mural P_{O_2} values and puncture depths can be used to calculate in vivo wall oxygen consumptions (w), using either a thin-walled model or a model in which medial thickness is a significant part of the luminal radius (see Appendix). These oxygen consumptions can then be inserted into the diffusion equation and "best-fit" profiles constructed and compared with the actual mural data points. We assumed that a fit within the limits of our measurement error would support the concept of transport purely by radial diffusion. Oxygen flux (j) within the wall near the borders of the media can be calculated and used as a secondary check on the accuracy of the original calculations. w values so obtained were also compared to wall stress calculations obtained through modification of standard stress formulations. The mathematics of these calculations are given also in the Appendix.

RESULTS

Data presented here were obtained from 10 experiments. Eight are discussed in greater detail, because more complete information was obtained. In seven, full histologic measurements permitted evaluation of the thick-walled diffusion model. For the group, averages and standard deviations were as follows: weight, 3.8±3 kg; Pa_{O_2}, 94±8 torr; Pa_{CO_2}, 38±10 torr; pH, 7.34±0.06; mean arterial pressure, 82±11 mm Hg; and internal arterial diameter, 930±130 μm.

Data published previously from this laboratory suggested a marked influence of the P_{O_2} level surrounding the rabbit femoral artery on the direction and contour of the P_{O_2} profile within the arterial tissue (14). An example of this phenomenon is shown in Fig. 2. At comparable levels of arterial oxygen tension and tissue oxygen consumption, a superfusion P_{O_2} of 93 torr completely altered the continuous downward trend in P_{O_2} between intima and adventitial surface which is present when the superfusion P_{O_2} is ~30 torr. This would also suggest to us a relative absence of effective vasa vasorum in the adventitia in this preparation.

If w were absent, the P_{O_2} profile would be linear

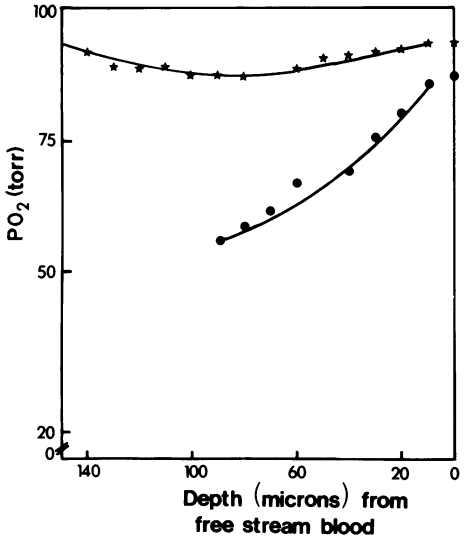

FIGURE 2 Data from arterial punctures with two different superfusion P_{O_2} levels, but similar blood P_{O_2} values. The lower curve was obtained with a superfusion P_{O_2} of ~30 torr, and represents points obtained from the arterial media. The upper curve was obtained with a superfusion level of 93 torr. Solid lines were obtained by back-fitting the diffusion equation, given the calculated mean value for oxygen utilization. Depth from free stream blood is approximate.

between intima and adventitia using the model for very thin-walled arteries, and very nearly so for vessels with thicker walls. The rather marked downward bowing of the curves seen in Fig. 2 is a reflection of w. Given the assumptions of the method, we examined its uniformity through the media in the following way. w was calculated as described in the Appendix, and this value was used to recalculate oxygen tension profiles for a theoretic curve of uniform w. This curve was superimposed on the actual data points and w was considered uniform if the data points corresponded to the theoretic curve within the limits of experimental error.

All necessary dimensions were available from freeze-exchange transverse histologic sections for seven cases and medial thickness could be compared to the length of the theoretic line fit. One such comparison is shown in Fig. 3. The oxygen tension profile is superimposed on a portion of the wall traversed, both adjusted to the same size scale. The fit would suggest that w was relatively constant through the media, although no histologic checks were available on electrode position. For the overall group, mean difference between histologic medial thickness and length of the profile of apparently uniform w was 8 μm. All tissue thicknesses were slightly smaller.

Fig. 4 is a composite of oxygen tension profiles showing actual data points on which are superimposed the theoretic curves of uniform w with calculations based on the thick-walled model. For the group, the fall

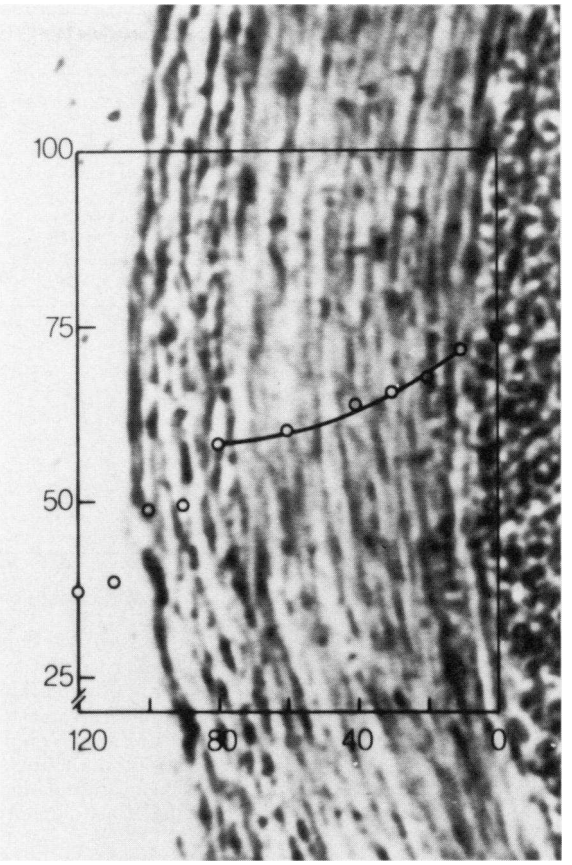

FIGURE 3 Photomicrograph of a freeze-exchanged transverse section of arterial wall, normalized in size to the superimposed oxygen tension profile; P_{O_2} (torr) on ordinate, distance from approximate position of the intima on abscissa. Erythrocytes to right, adventitia on the left. The clear space on the left was covered by superfusion during the experiment. In all experiments, values of P_{O_2} had a relatively smooth contour in the region approximately corresponding to the media, shown by the continuous line. Small circles represent measured P_{O_2} values.

in P_{O_2} from free stream blood to medial-adventitial border was 21±6 torr and lowest medial P_{O_2} was 62±14 torr. In each case, the fit appears adequate within the limits of experimental error.

These may be compared with the same display as calculated according to the thin-walled model, which is shown in Fig. 5, and there is little difference based on observation. However, if the wall is sufficiently thin in relation to lumen radius the solutions for each model are the same and there should be no significant difference in calculated w. Theoretically, if the thick-walled model is more appropriate, w so calculated should be the lesser values.

w values calculated by the two methods are compared in Fig. 6. The mean for the group calculated by the thin-wall theory was 136±48 vs. 99±30 nl_o/ml-s

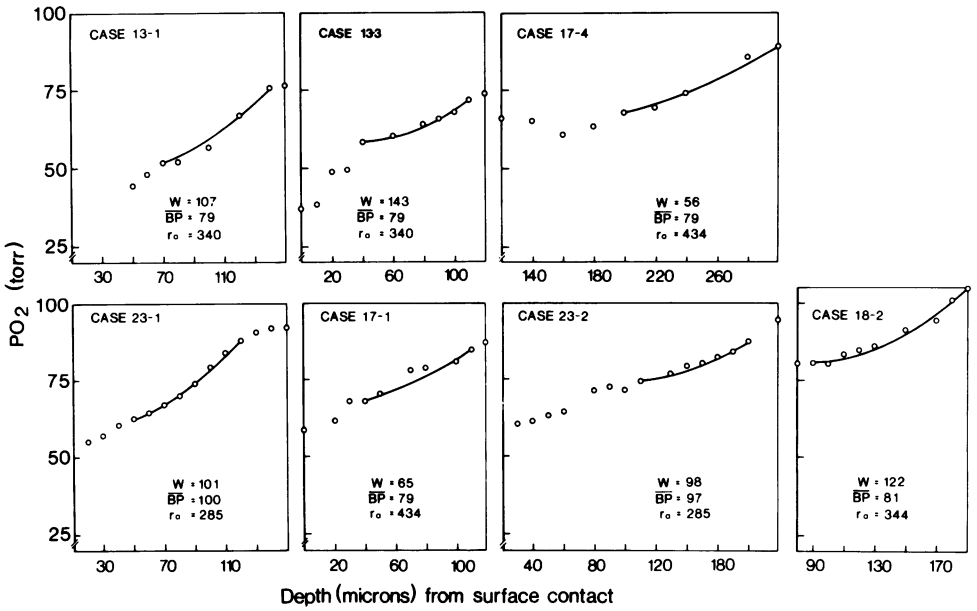

FIGURE 4 Oxygen partial pressure vs. depth of puncture from adventitial electrode contact. Superfusion P_{O_2} ~30 torr in each case. Because a varying adventitial thickness was present which could not be distinguished from possible fibrin deposition, and the general trend in these areas was similar, complete outer profiles are not shown. Circles are measured P_{O_2} levels. The solid lines represent theoretic curves of uniform oxygen consumption, and were derived only from measurements in the media, as described in the text. w is oxygen consumption (nanoliters of oxygen per milliliter per second); $\overline{BP}$ is mean arterial blood pressure; r_a is internal arterial radius in microns, as obtained from freeze-exchanged histologic sections.

for thick-wall theory, although the values are clearly correlated. This difference was significant (paired t test, $P < 0.001$).

As noted in the Appendix, these values do not depend on an explicit knowledge of j to the intimal surface or away from the adventitial surface, although j

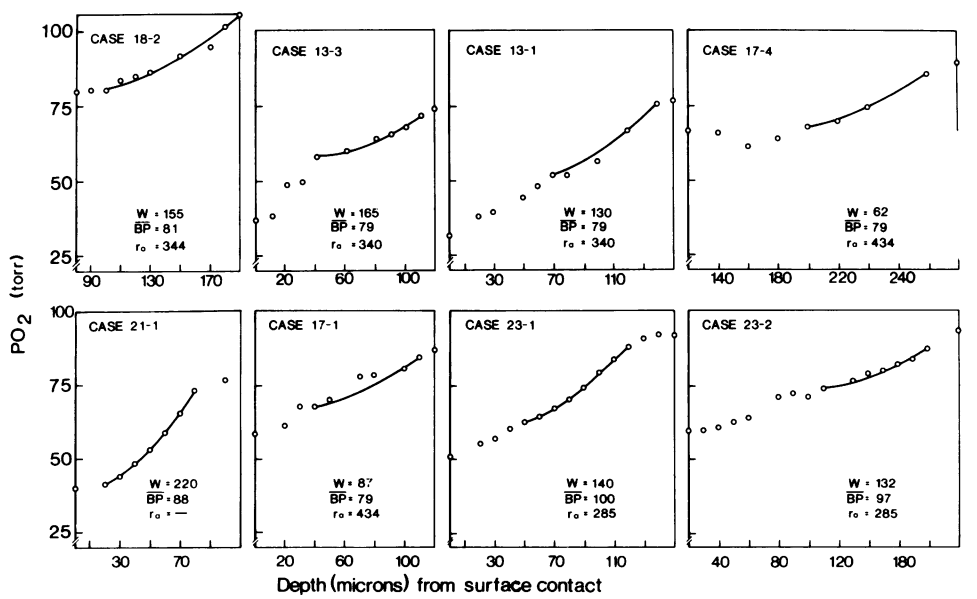

FIGURE 5 Notation as in Fig. 4, except that the continuous curves were obtained using the thin-wall (plane unidimensional diffusion) model.

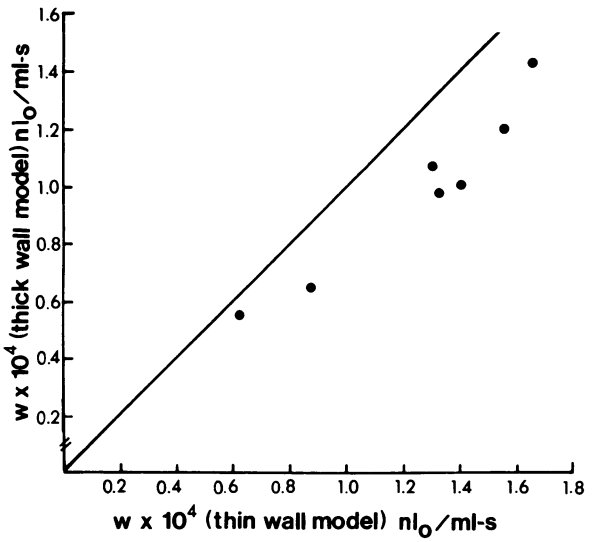

FIGURE 6 Medial oxygen consumption calculated according to thick- and thin-wall models. Although the theoretic fits cannot be distinguished from each other, calculations based on the thick-walled model are lower than those based on the thin; this is expected when the wall thickness is a significant portion of the arterial radius. Therefore, the thick-wall model is the more appropriate.

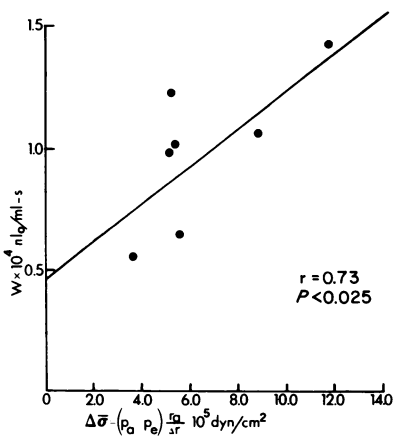

FIGURE 7 Mean latitudinal differential wall stress ($\Delta\bar{\sigma}$) on the abscissa, w on the ordinate. p_a is total arterial pressure, p_e is external pressure, r_a is inner wall radius, and Δr is medial thickness. ($p_a - p_e$) is, for practical purposes, intra-arterial pressure as it is usually measured.

in closely adjacent points within the media (r_o and r_i) can be calculated by Eq. 7 in the Appendix. Doing so, average j within the wall near the intima (j_o) was 1.2 nl_o/cm^2-s, and near the adventitia (j_i), 0.21 nl_o/cm^2-s.

As a check on these values, w was calculated from j values obtained (Appendix). w so determined was 110 nl_o/ml-s, as compared to the direct calculations of 99 nl_o/ml-s for thick-wall theory. An approximate test can be derived from thin-wall theory and produced values 10% higher.

There was no clear relationship between arterial pressure or internal radius and w separately, probably because pressures and radii were similar in this group of animals. In attempting to compare wall stress ($\Delta\bar{\sigma}$) and w the following factors led to our choice of dimensions used in the stress formulation. There was considerable circumferential variability in the thickness of the adventitia (but not media), and the adventitia merged into surrounding tissue. Using average adventitial thickness plus medial thickness as an estimate of total wall thickness in each case, there was not a clear relationship between the latter and medial w ($P \simeq 0.08$). The media is likely to be the dominant load-bearing element in a vessel which is not overstretched. Because measurable w was limited to the media, any relation between wall w and $\Delta\bar{\sigma}$ should be closely related to the behavior of the media. Therefore, medial thickness was chosen as our best estimate of effective wall thickness in calculating $\Delta\bar{\sigma}$ for comparison with medial w (Fig. 7), and a positive relationship was found ($P = 0.025$). To the extent that any fraction of wall stress is supported by elements other than smooth muscle, the slope of the relationship would probably be underestimated.

DISCUSSION

The oxygen tension profiles we obtained from rabbit femoral arterial walls are different from previous profiles reported for in vivo experiments. Specifically, both previous in vivo studies from normal animals showed an abrupt increase in oxygen current or P_{O_2} over a short distance on traversing the region of the intima into arterial blood (8, 9). Our profiles in this region were continuous, rising progressively to that of arterial blood as the wall was crossed from adventitia to lumen. Near the intima, our findings were similar to in vitro studies of excised arterial wall reported by Schneiderman et al. (10) and by Jurrus and Weiss (11).

However, previous studies, both in vivo and in vitro, showed lowest values for P_{O_2} in the region of the central inner media. Adventitial values were higher, suggesting that vasa vasorum might provide a considerable source for oxygenation of the outer layers of the media. Our profiles decline progressively from arterial blood to adventitia. It is appropriate therefore to compare experimental techniques and the animal preparations used in these various studies in an attempt to bridge the gap that now exists between in vitro and in vivo studies.

Arterial wall thickness. The average thickness of the media in our rabbit femoral arteries was 72 μm, as measured after *in situ* freezing and freeze-exchange processing. Moss et al. (8) did not directly report wall thickness in their dog femoral arteries and their oxygen current measurements cannot be interpreted in units of

oxygen tension, so no direct comparisons can be made. Niinikoski et al. (9) used rabbit abdominal aortas in which the average electrode advance required to traverse the wall was 173 μm. Schneiderman et al. (10) and Jurrus and Weiss (11) used rabbit thoracic aortas. The latter investigators reported an average wall thickness of 483 μm in normal vessels. The minimum P_{O_2} measured in any arterial wall must depend on an interaction between P_{O_2} inside the lumen and surrounding the adventitia, vasal supply, rate of medial w, local diffusion coefficients, and the overall thickness of the media. Of the several possible factors, a very thin media is the only identifiable one accounting for the fact that our lowest medial P_{O_2} level (average 62 torr) was higher than those reported in previous studies. A suggestion of this may be obtained analytically by "allowing" our arterial walls to thicken, simply by a change in boundary conditions in the diffusion equation. In this analysis, w and arterial blood P_{O_2} from each of our experiments were held constant, arterial blood was considered to be the only effective oxygen source (any adventitial supply was considered too remote to affect the analysis near the intima), and the effect of increasing wall thickness was examined by calculation. Using arterial P_{O_2} and wall w values from each animal and taking averages, a P_{O_2} of ~20 torr would have been reached at 156±30 μm. This may be unrealistic in that all variables are excluded except wall thickness. However, the direction of the result appears comparable to that directly measured by Jurrus and Weiss (11). They found a P_{O_2} of 27 torr at 223 μm from the intimal surface in minimally diseased vessels, and our average blood P_{O_2} was ~50 torr less than that of the superfusion fluid they used.

Vasa vasorum and periarterial environment. In our experiments we surrounded the adventitial surface of the artery with a flowing solution at 30 torr P_{O_2}, the value we had measured in tissue surrounding the arterial wall. We chose to do this for reasons stated earlier. Therefore, the general shape of our profiles, which lacked a rise in P_{O_2} at the medial-adventitial boundary, suggested that our arteries had no effective vasa vasorum. This is clearly different from all previous reported results and again, a comparison of methodology and animal models must be made. The conditions we used external to the artery were also different than those in previous studies. Moss et al. (8) apparently left the artery exposed to room air. Thus, atmospheric contamination or differential temperature effects on electrode response could account for the high P_{O_2} levels at the adventitia, and we cannot evaluate the presence or absence of an effective vasal supply of oxygen from their profiles. Although the puncture sites in the experiments of Niinikoski et al. (9) were covered with a drop of mineral oil, the same argument may be made nearly as strongly. On the other hand, Schneiderman et al. (10) used an experimental arrangement which perfused the intimal surface of the aorta with a P_{O_2} in solution of ~144 torr, and the proximal intercostals were intact, so that any vasa vasorum were also probably perfused with the same solution. Jurrus and Weiss (11) perfused both sides of the excised vessel with solutions at ~144 torr P_{O_2}. The presence of vasa vasorum is compatible with these observations but interaction with the high adventitial side P_{O_2} cannot be excluded, particularly in the latter paper; the tissue was compressed except for the millimeter surrounding the puncture site, and functional vasa were not perfused or necessarily preserved.

It seems likely to us that arterial size in relation to vasal distribution must be taken into account in evaluating the difference between our profile shapes in the area of the adventitia in comparison to those of previous workers. In examining species differences in the medial distribution of aortic vasa vasorum in mammals, Wolinsky and Glagov (21) found that the media was completely avascular until its thickness approached 400 μm. This does not exclude diffusion from adventitial vessels but would suggest that our very thin walls had no vasa vasorum (none were seen on examination). By comparison, vasa vasorum at least at the adventitial-medial junction, may have been present in the thicker rabbit aortas used in three of the previous studies.

In our experiments, artefactual observations as a result of the necessities of the surgical exposure cannot be excluded completely; however, care was taken not to injure the adventitia. There is also the possibility that the electrodes in our study compressed any capillaries present and induced a behavior appropriate for vessels which have no capillaries. This explanation seems unlikely, because evidence of an adventitial oxygen supply is usually present in profiles from dog femoral arteries.[2] In these, the profiles are often triphasic, rising from superfusion fluid level to intermediate values in the region of the adventitial-medial boundary, falling again toward the mid-media, then rising progressively and smoothly to luminal blood levels as the wall is traversed from adventitia to luminal blood.

Is there a relative diffusional barrier in the tissue at or near the intima? Although scaling is different for reasons mentioned above, our profiles resembled those of Schneiderman et al. (10) and of Jurrus and Weiss (11) in the inner parts of the wall, in that there was a smooth rise rather than discontinuous abrupt rise in P_{O_2} in this area. The results of our calculations, based on diffusional theory, are compatible with relatively uniform values for w and diffusion coefficient near the luminal portion of the media. We discuss here technical differ-

[2] Unpublished observations.

ences which may have caused our profiles to resemble previous profiles obtained in vitro, and not those in vivo. We used the recessed-tip glass microcathode of the Whalen type as did Jurrus and Weiss (11) in an in vitro study. Although the electrode form can be varied somewhat by the fabrication technique, our tips were small, in the range of 3–5 μm, and sharply beveled by grinding to a fraction of a micron. A glass-pulling technique was arranged so that the taper was gradual. However, in vivo, it was very difficult to puncture the wall without visible indentation or fracture of the shaft. When indentation of the wall occurred, steady or decreasing oxygen currents were obtained. With further advancement, luminal puncture occurred suddenly with an abrupt, discontinuous rise in P_{O_2}. It is noteworthy that this phenomenon often occurred when the electrode had reached a depth corresponding to the region of the internal elastic lamina. For this reason all data reported here were obtained with a longitudinally vibrating electrode. Using this technique, surface indentation was not produced in the experimental results shown here, and the profiles are smooth. When surface indentation was identified, the electrode was withdrawn and cleaned and a puncture then started in an adjacent location. Moss et al. (8) used a very large wire electrode which we would expect to produce significant tissue deformation. The type of electrode used by Niinikoski et al. (9) was apparently sharper, but no vibration was used. On the other hand, Schneiderman et al. (10) used an oblique rather than perpendicular puncture technique. This may well have prevented significant compression. Jurrus and Weiss (11) supported tissue between two coverslips containing matched 1-mm holes through which the traverses were made. This support system may also have prevented significant tissue indentation within the course of the puncture.

Type of electrode. We used a recessed-tip metal-filled glass microcathode of the Whalen type. Schneiderman and Goldstick (15) have recently reviewed electrode characteristics necessary for adequate measurement of tissue P_{O_2}, and have demonstrated, in a mathematical study, the desirability of a recessed cathode. Whalen and others (22–25) have demonstrated the usefulness of this design in studies of tissue oxygenation. There are several advantages. This type of electrode demonstrates no stirring artefact and can be calibrated equivalently in solution or tissue. Because the recess contains nearly all of the diffusion field produced by oxygen consumption at the cathodal surface, essentially no diffusion field produced by the electrode is present in tissue. Therefore tissue P_{O_2} is probably more accurately measured than by a membrane-covered surface. In our modification, the recess is filled with a hydrogel which is permeable to oxygen but impervious to protein. This appears to be responsible for the near absence of cathodal poisoning. The previous in vitro arterial wall study of Jurrus and Weiss (11) made use of the advantageous characteristics of this electrode design.

Oxygen consumption, wall structure, and stress. To our knowledge, there has been no previous report of the determination of arterial wall oxygen utilization from in vivo data using the appropriate thick-wall model. By contrast, numerous respirometer values at 37°C for various types of vascular tissue segments have been reported. Exact comparison is difficult because reported values are often referred to dry tissue weight. To make an approximate comparison, we have assumed tissue weight of 1.06 g/ml, with a water content of 75% (26, 27). Using these values when necessary, representative results are 20 nl_o/cm^3-s wet tissue in human umbilical arteries (28); 50 nl_o/cm^3-s in bovine mesenteric veins (29); 57 and 71 nl_o/cm^3-s in rabbit aortas (5, 11); and 110–230 nl_o/cm^3-s in resting and stimulated dog femoral artery segments (30). Our mean value of 99 and range of 56–142 nl_o/cm^3-s appear reasonable with respect to these respirometer studies.

In situ freezing of the arterial segment during life followed by freeze-exchange processing in the regions of the electrode traverses does not guarantee preservation of the exact dimensions present during the experiment, but appears to provide the best representation reasonably available (31). Because electrode contact with the adventitial surface was easily defined within a few microns, oxygen tension profiles could be compared with the histologic sections. The close correspondence between histologic medial thickness and the portion of the oxygen tension profile compatible with uniform w suggests that there are not large differences in diffusion coefficient or w in these relatively thin muscular walls, and that wall deformation produced by electrode advance was not a great problem.

The media is not homogeneous, so our global calculations must be assumed to show some mean value for the local tissue w. The solution of the diffusion equation permits differential calculation of w over small portions of each profile by changing the boundary conditions. There appeared to be no advantage to this, because the assumption of a uniform w through the media of these thin arteries led to profile fits within the experimental error of the method.

In calculating w values for the diffusion and solubility coefficients had to be assumed. The diffusion coefficient for rabbit femoral arteries has apparently not been measured, but in a normal artery of this size, the intima is extremely thin and probably contributes very little to an overall average. The value we used for the diffusion coefficient (10^9 nm^2/s) was rounded off from that measured by Kirk and Laursen (32) in postmortem human arteries, although they found variation between cases and a slight difference between inner and outer layers (intima $\simeq 0.84 \times 10^9$ nm^2/s, media

$\simeq 0.96 \times 10^9$ nm²/s). Had we used their average value for the media, our calculated w would be 4% lower than the values given. Our solubility coefficient (30 nl_o/cm^3-torr) is similar to that reported for many tissues of similar composition.

Consideration of a possible relationship between medial w and wall stress is difficult. An unknown portion of the stress is supported by passive medial and adventitial elements, but it was of interest to search for such a relationship because of in vitro demonstrations of a relation between smooth muscle force and w (29, 30). In the cases in which histologic sections were available, stress was therefore calculated (Appendix, Eq. 13). Consistent with the notion of active muscular force, medial thickness rather than wall thickness was used in these calculations. The positive relationship resulting is clearly shown in Fig. 7. There is also a tensile stress in the arterial wall in the longitudinal direction, but its magnitude is not known for these experiments.

We have attempted to resolve the disparity between previous in vivo and in vitro studies of arterial wall oxygenation. We believe we have provided evidence that the discontinuities in oxygen tension reported in the in vivo studies, but not in vitro studies, are probably compressional artefacts, and are not usually present within normal arterial walls. We consider it likely that we found no evidence for the presence of vasa vasorum in our studies because of the thinness of these rabbit femorals, and that evidence of a vasal oxygen supply in previous in vivo studies is compatible with the size of the larger arteries used. However, the unusual environmental conditions present outside the adventitia in the previous experiments make interpretation difficult. It appears that an understanding of arterial wall oxygenation in vivo requires both careful specification of periarterial environment, and maintenance of luminal blood flowing under normal conditions, which we have done. We have, in addition, presented calculations showing that medial oxygenation under the conditions of our study can be attributed purely to diffusion, and have demonstrated calculations of in vivo medial w and mural flux, derived from diffusional theory. These values corresponded closely to values previously measured by respirometer in vitro.

ACKNOWLEDGMENTS

The authors are grateful to Mr. Greg Lippert, and Mss. Jackie Velten, Amanda Marmolejo, and Monica Velez for extensive technical assistance and to Mrs. Diane Austin who rendered invaluable secretarial assistance.

This work is supported by National Institutes of Health grants HL 18969 and NL 21032.

APPENDIX

If arterial blood and periarterial Po_2 levels, wall dimensions, mural w, and diffusion coefficient are constant over the time interval and area measured, and diffusion is unidimensional, then the appropriate diffusion equation within a tubular unbending arterial wall is (33)

$$0 = -\frac{1}{r}\frac{d}{dr}(rj) - w, \tag{1}$$

where r is the radius to the point of measurement; j is the oxygen flux (nanoliters of oxygen per square centimeter per second) and w is the oxygen consumption (nanoliters of oxygen per milliliter per second). j is related to oxygen concentration gradient by Fick's Law:

$$j = -D(dc/dr) \tag{2}$$

where D is the diffusion coefficient.

Substitution of Fick's Law into the diffusion equation gives the following differential equation that governs the variation of oxygen concentration c (nanoliters of oxygen per cubic centimeter) in the arterial wall

$$\frac{d^2c}{dr^2} + \frac{1}{r}\frac{dc}{dr} = \frac{w}{D}. \tag{3}$$

This equation was solved for the conditions that at some distance r_o from the axis of the vessel, within the wall but near the intima, the oxygen concentration is c_o; and at larger distance r_i from the axis of the vessel, still within the tunica media, the oxygen concentration is c_i. The solution of the differential equation for the oxygen concentration c at radius r between r_o and r_i for these conditions and uniform w is:

$$\frac{(c_o - c)\ln(r_i/r_o)}{(c_o - c_i)\ln(r/r_o)} = 1 + \frac{1}{4}\frac{w}{D}\frac{r_o^2}{(c_o - c_i)}\left\{\left[\left(\frac{r_i}{r_o}\right)^2 - 1\right] - \frac{\ln(r_i/r_o)}{\ln(r/r_o)}\left[\left(\frac{r}{r_o}\right)^2 - 1\right]\right\} \tag{4}$$

where the diffusion coefficient D was taken as 10^9 nm²/s (32) and the oxygen concentration c within the wall is related to the oxygen partial pressure Po_2 as $c = SPo_2$, where S is the oxygen solubility coefficient, taken as 30 $nl_o/(cm^3\text{-torr})$.

In relation to the left-hand side of Eq. 4 (y value), 1 is the intercept and the constant term $wr_o^2/4D(c_o - c_i)$ may be taken as the slope N_i. This was determined by the least-squares method and w was calculated as:

$$w = (4N_iD(c_o - c_i))/r_o^2. \tag{5}$$

In that the equation does not include convective transport within the tissue of the wall, we assumed that a good fit would tend to exclude this as an important mechanism for oxygen transport within the wall. This assumption is supported in a previous paper by Back (33). For this purpose, having obtained a best overall value for w, a best-fit line was placed through the data points by selecting increments of r and using the solution of the diffusion equation in the form:

$$c = c_o + \left\{\frac{(c_o - c_i) - \frac{1}{4}\frac{w}{D}(r_o^2 - r_i^2)}{\ln(r_o/r_i)}\right\}\ln\frac{r}{r_o} - \frac{1}{4}\frac{w}{D}(r_o^2 - r^2). \tag{6}$$

This solution of the diffusion equation allows for the diffusional exchange of oxygen between the outer surface of

the vessel and the superfusion fluid because the oxygen fluxes either at the inner or outer arterial wall surfaces are not imposed as boundary conditions in the solution of the diffusion equation. Rather, the oxygen concentration c_o and c_i and radii r_o and r_i, respectively, are used as determined from the experiments. The local oxygen flux j at radius r can be determined by differentiation of Eq. 6 as:

$$j = -D\left\{\left[\frac{(c_o - c_i) - \frac{1}{4}\frac{w}{D}(r_o^2 - r_i^2)}{\ln\left(\frac{r_o}{r_i}\right)}\right]\frac{1}{r} + \frac{1}{2}\frac{w}{D}r\right\}. \quad (7)$$

As a check on flux values so calculated, the values were then used to retrieve w, because

$$\frac{1}{r}\frac{d}{dr}(rj) = -w \quad \text{and} \quad \int d(rj) = -\int_{r_o}^{r_i} wrdr$$

Integrating and rearranging, with $\Delta r = r_i - r_o$:

$$w = \frac{2[r_o(j_o - j_i) - \Delta r j_i]}{2\Delta r r_o + \Delta r^2}. \quad (8)$$

If the arterial wall is very thin in relation to the radius of the vessel, solution of the diffusion equation takes the form

$$\frac{(c_o - c)}{(c_o - c_i)}\left(\frac{n_i}{n}\right) = 1 + \frac{1}{2}\frac{w}{D}\frac{n_i^2}{(c_o - c_i)}\left(1 - \frac{n}{n_i}\right), \quad (9)$$

the terms defined as before except that n is some arbitrary distance corresponding to measured c, between $n_o = 0$ and n_i. In this case, $N_2 = (w/2D)(n_i^2)/(c_o - c_i)$ is the slope of the linear relation between $((c_o - c)/(c_o - c_i))(n_i/n)$ and n/n_i, and $w = 2DN_2(c_o - c_i)/n_i^2$. This simpler model was also tested for fit in each case.

It was of interest to search for a relationship between w, arterial pressure, vessel radius, and wall thickness. The average value for latitudinal (tangential) stress $\bar{\sigma}$ distributed across the vessel wall is given as follows (34, 35)

$$\bar{\sigma}\Delta r = p_a r_a - p_e r_e, \quad (10)$$

where p_a is the mean arterial pressure, p_e is the external pressure, r_a and r_e are the inner and outer wall surface radii and Δr is the wall thickness, $r_e - r_a$. This relationship can be more conveniently written as

$$\bar{\sigma} = \Delta p \frac{r_a}{\Delta r} S \quad (11)$$

where

$$S = 1 - \frac{p_e}{\Delta p}\frac{\Delta r}{r_a} \quad (12)$$

and Δp is the mean arterial pressure above ambient pressure.

This latitudinal stress may be a tension or a compression depending upon whether $p_a r_a$ is larger or smaller than $p_e r_e$. However, the active latitudinal stress descriptive of the force which the smooth muscle cells work against is believed to be the difference between the latitudinal stress and that which would exist if the pressure in the vessel were the same as the surroundings, i.e.,

$$\Delta\bar{\sigma} = (p_a - p_e)\frac{r_a}{\Delta r}. \quad (13)$$

In the cases in which histologic sections were available, $\Delta\bar{\sigma}$ was so calculated, and consistent with the concept of active stress, the medial thickness was used as an estimate of Δr.

REFERENCES

1. Adams, C. W. M., and O. B. Bayliss. 1969. The relationship between diffuse intimal thickening, medial enzyme failure and intimal lipid deposition in various human arteries. *J. Atheroscler. Res.* **10:** 327–339.
2. Lehninger, A. L. 1959. The metabolism of the arterial wall. *In* The Arterial Wall—Aging, Structure, and Chemistry. A. L. Lansing, editor. Williams & Wilkins Company, Baltimore. 220–246.
3. Zemplenyi, T. 1968. Arterial hypoxia and lactate dehydrogenase isozymes as related to atherosclerosis. *In* Enzyme Biochemistry of the Arterial Wall as Related to Atherosclerosis. Lloyd-Luke Ltd., London. 161–167.
4. Kirk, J. E., P. G. Effersoe, and S. P. Chiang. 1954. The rate of respiration and glycolysis by human and dog aortic tissue. *J. Gerontal.* **9:** 10–35.
5. Morrison, A. D., L. Berwick, L. Orci, and A. I. Winegrad. 1976. Morphology and metabolism of an aortic intima-media preparation in which an intact endothelium is preserved. *J. Clin. Invest.* **57:** 650–660.
6. Kjeldsen, K., J. Wanstrup, and P. Astrup. 1968. Enhancing influence of arterial hypoxia on the development of atheromatosis in cholesterol-fed rabbits. *J. Atheroscler. Res.* **8:** 835–845.
7. Hugod, C., L. H. Hawkins, K. Kjeldsen, H. K. Thomsen, and P. Astrup. 1978. Effect of carbon monoxide exposure on aortic and coronary intimal morphology in the rabbit. A revaluation. *Atherosclerosis.* **30:** 333–342.
8. Moss, A. J., P. Samuelson, C. Angell, and S. I. Minken. 1968. Polarographic evaluation of transmural oxygen availability in intact muscular arteries. *J. Atheroscler. Res.* **8:** 803–810.
9. Niinikoski, J., C. Heughan, and T. K. Hunt. 1973. Oxygen tensions in the aortic wall of normal rabbits. *Atherosclerosis.* **17:** 353–359.
10. Schneiderman, G., T. K. Goldstick, and L. Zuckerman. 1974. Similarity between the site of minimum pO_2 and the site of initiation of atherosclerosis. *Proc. 27th Ann. Conf. Eng. Med. Biol. Alliance Eng. Med. Biol.* **16:** 283.
11. Jurrus, E. R., and H. S. Weiss. 1977. In vitro tissue oxygen tensions in the rabbit aortic arch. *Atherosclerosis.* **28:** 223–232.
12. Whalen, W. J., J. Riley, and P. Nair. 1967. A microelectrode for measuring intracellular pO_2. *J. Appl. Physiol.* **23:** 798–801.
13. Whalen, W. J., P. Nair, and R. A. Ganfield. 1973. Measurements of oxygen tension in tissues with a micro oxygen electrode. *Microvasc. Res.* **5:** 254–262.
14. Kanabus, E. W. 1977. Oxygen availability and utilization in the arterial wall: an in vivo microelectrode study. Ph.D. Dissertation, University of Southern California, Los Angeles. 1–144.
15. Schneiderman, G., and T. K. Goldstick. 1978. Oxygen electrode design criteria and performance characteristics: recessed cathode. *J. Appl. Physiol. Respir. Environ. Exercise Physiol.* **45:** 145–154.
16. Duling, B. R., and E. Staples. 1974. A comparison of the performance of microvessels in the hamster cheek pouch during exposure to tris and biocarbonate buffers. *Microvasc. Res.* **7:** 277–279.
17. Bates, M. L., A. Feingold, and M. I. Gold. 1975. The ef-

fect of anesthetics on an in vivo oxygen electrode. *Am. J. Clin. Pathol.* **64:** 448–451.
18. Severinghaus, J. W. 1966. Blood gas calculator. *J. Appl. Physiol.* **21:** 1108–1116.
19. Kanabus, E. W., C. Feldstein, and D. W. Crawford. 1977. A vibrating device to aid in inserting microelectrodes into tissue. *Fed. Proc.* **36:** 524. (Abstr.)
20. Sobin, S. S., S. Bernick, H. M. Tremer, T. H. Rosenquist, R. Lindal, and Y. C. Fung. 1974. The fibroprotein network of the pulmonary interalveolar wall. *Chest.* **65:** 4S–5S.
21. Wolinsky, H., and S. Glagov. 1967. Nature of species differences in the medial distribution of aortic vasa vasorum in mammals. *Circ. Res.* **20:** 409–421.
22. Gore, R. W., and W. J. Whalen. 1968. Relations among tissue pO_2, qO_2, and resting heat production of frog sartorius muscle. *Am. J. Physiol.* **214:** 277–286.
23. Whalen, W. J. 1971. Intracellular pO_2 in heart and skeletal muscle. *Physiologist.* **14:** 69–82.
24. Whalen, W. J., J. Savoca, and P. Nair. 1973. Oxygen tension measurements in carotid body of the cat. *Am. J. Physiol.* **225:** 986–991.
25. Whalen, W. J., P. Nair, D. Buerk, and C. A. Thuning. 1974. Tissue pO_2 in normal and denervated cat skeletal muscle. *Am. J. Physiol.* **227:**
26. Spector, W. 1956. Handbook of Biological Data. W. B. Saunders Company, Philadelphia.
27. Altman, P. H., and D. S. Dittmer. 1971. Respiration and Circulation. Federation of American Societies for Experimental Biology, Bethesda. 16–22.
28. Colthart, C., and M. R. Roach. 1970. The effect of temperature on the oxygen consumption of isolated human umbilical arteries. *Can. J. Physiol. Pharmacol.* **48:** 377–381.
29. Paul, R. J., J. W. Peterson, and S. R. Caplan. 1973. Oxygen consumption rate in vascular smooth muscle: relation to isometric tension. *Biochim. Biophys. Acta.* **35:** 474–480.
30. Kosan, R. L., and A. B. Burton. 1966. Oxygen consumption of arterial smooth muscle as a function of active tone and passive stretch. *Circ. Res.* **18:** 79–88.
31. Sobin, S. S., and T. H. Rosenquist. 1973. Determination of dimensions and geometry in fixed specimens. *Microvasc. Res.* **5:** 271–284.
32. Kirk, J. E., and T. J. S. Laursen. 1955. Diffusion coefficients of various solutes for human aortic tissue with special reference to variation in tissue permeability with age. *J. Gerontol.* **10:** 288–302.
33. Back, L. H. 1976. Analysis of oxygen transport in the avascular region of arteries. *Math. Biosci.* **31:** 285–306.
34. Fung, Y. C. 1968. Biomechanics: Its scope, history, and some problems with continuum mechanics in physiology. *Appl. Mech. Rev.* **21:** 1–20.
35. Bergel, D. H. 1972. Properties of blood vessels. *In* Biomechanics Its Foundation and Objectives. Y. C. Fung, N. Perrone, and M. Anliker, editors. Prentice-Hall, Inc., Englewood Cliffs, N. J. 105–139.